Journal of
Instrumentation

TCAD modeling of bulk and surface radiation damage effects in silicon devices

Published by IOP Publishing for Sissa Medialab

Received: *May 14, 2025*
Revised: *July 18, 2025*
Accepted: *August 13, 2025*
Published: *September 10, 2025*

20th Anniversary Trento Workshop on Advanced Silicon Radiation Detectors
Trento, Italy
4–6 February 2025

TCAD modeling of bulk and surface radiation damage effects in silicon devices

F. Moscatelli[a,b,*] **A. Morozzi**[b] **T. Croci**[b] **D. Passeri**[c,b] **K. Aouadj**[b] **V. Sola**[d] **G.-F. Dalla Betta**[e] **and A. Fondacci**[f,b]

[a] *CNR-Istituto Officina dei Materiali (IOM), via A. Pascoli, Perugia, Italy*
[b] *INFN Perugia, via A. Pascoli, Perugia, Italy*
[c] *Department of Engineering, University of Perugia, via G. Duranti 93, Perugia, Italy*
[d] *Department of Physics, University of Torino, via P. Giuria 1, Torino, Italy*
[e] *Department of Industrial Engineering, University of Trento, via Sommarive 9, Trento, Italy*
[f] *Department of Physics, University of Perugia, via A. Pascoli, Perugia, Italy*

E-mail: moscatelli@iom.cnr.it

Abstract: Future frontier accelerators envision the use of silicon sensors in environments with fluences exceeding 1×10^{17} 1 MeV n_{eq}/cm^2. Presently available silicon sensors can operate efficiently up to fluences of the order of 10^{16} 1 MeV n_{eq}/cm^2. Therefore, novel sensors and readout electronics must be developed. Within this framework, state-of-the-art Technology CAD (TCAD) tools can be proficiently used to account for both bulk and surface radiation-induced damage effects in semiconductor sensors, fostering design optimization and enabling a predictive insight into the electrical behaviour of novel solid-state detectors. In particular, the balance between extending already developed models and methodologies or devising different approaches should be carefully considered. In this contribution, the different available TCAD numerical models addressing bulk and surface radiation damage effects will be illustrated. It will also be shown how these models have been used for the optimization of devices, particularly 3D sensors and Low Gain Avalanche Diodes. Moreover, extending the applicability of these models to extreme fluence scenarios requires carefully accounting for the modeling of acceptor and donor removal, impact ionization, carrier mobility and lifetime, and trap dynamics.

Keywords: Detector modelling and simulations II (electric fields, charge transport, multiplication and induction, pulse formation, electron emission, etc); Particle tracking detectors (Solid-state detectors); Radiation-hard detectors; Timing detectors

*Corresponding author.

https://doi.org/10.1088/1748-0221/20/09/C09006

2025 JINST 20 C09006

Contents

1 Introduction

Next-generation high-energy particle colliders, designed for fundamental physics research, will require ultra-precise tracking in both space and time, presenting formidable challenges in terms of energy and luminosity demands. In these environments, tracking detectors are expected to withstand extreme radiation levels, requiring extensive research and development to enhance their radiation tolerance and extend operational limits as far as possible. The detectors and electronics used for the High Luminosity Large Hadron Collider (HL-LHC) scenario will therefore no longer be applicable, and the study of the effects of radiation damage will become even more important.

In this context, state-of-the-art Technology CAD (TCAD) tools [1, 2] will play a fundamental role in optimizing the sensors to be developed, taking into account the effects of radiation damage. Several numerical models [3–6] have been developed over the years to study and predict the behavior of specific sensors irradiated with different particles up to the relevant fluences for the HL-LHC upgrade. However, these existing models, need to be extended to accurately predict behavior at extreme fluences ($>1 \times 10^{17}$ 1 MeV equivalent neutrons per square centimeter, n_{eq}/cm^2). This is crucial to foster design optimization and to enable predictive insight into the electrical behavior of novel solid-state detectors. The ultimate goal is to simultaneously reproduce and predict the macroscopic electrical behavior of silicon detectors in terms of Current-Voltage (I-V), Capacitance-Voltage (C-V), and Charge Collection Efficiency (CCE) as a function of the voltage, at the fluences of interest in future collider experiments.

2 Radiation damage in silicon sensors

The high fluences in the HL-LHC and future collider experiments introduce defects both in the silicon substrate (bulk damage) and in the SiO_2 passivation layer, which affect sensor performance through the interface with the silicon bulk (surface damage). The main macroscopic effects of bulk damage on silicon detectors irradiated by hadrons are the change of the effective doping concentration N_{eff}, the increase in the leakage current and the trapping of free carriers, which reduces the Charge Collection Efficiency (CCE) [7]. At very high fluences, the depletion voltage (from $1/C^2$ measurement) can increase so much that the device cannot be completely depleted before reaching the breakdown,

2025 JINST 20 C09006

reducing the charge collection efficiency of the sensor. Beyond a fluence of 1×10^{16} n_{eq}/cm^2, the severe trapping of free carriers by radiation-induced defect levels can limit the silicon detector operation.

Changes in semiconductor properties at extreme fluences are fundamental to detector design and optimization, yet still poorly understood. A straightforward extrapolation of damage parameters to higher fluences is not possible due to the non-linear nature of defect formation with fluence [8, 9]. Furthermore, it is very important to consider the saturation of radiation damage effects above 5×10^{15} n_{eq}/cm^2 [10]. To better understand the limitations of the developed models, a thorough characterization of radiation effects at extreme fluences is essential. This will involve studying the radiation-induced defects using Deep-Level Transient Spectroscopy (DLTS), Thermally Stimulated Current (TSC), and Thermally stimulated capacitance (TSCap) spectroscopic techniques [11]. In TCAD simulations, we employ models to approximate the complex reality of radiation-induced defects. The information related to the defects (energy level, introduction rate, capture cross sections for example) extracted from these measurements serve as input parameters for TCAD simulations. However, characterizing defect parameters at fluences exceeding 1×10^{16} n_{eq}/cm^2 presents a challenge, necessitating suitable techniques for detecting defect parameters.

Sensors featuring innovative designs and distinctive features have attracted much interest in recent years to improve the radiation hardness of silicon sensors for future experiments. 3D detectors [12] represent an important option for their high CCE and very low time resolution even after very high fluences. Furthermore, due to the intrinsic charge multiplication, low-gain avalanche diode (LGAD) based devices emerge as another optimal candidate for this purpose. In this direction, new challenges need to be addressed to extend the charge carrier multiplication up to 1×10^{17} n_{eq}/cm^2. For these reasons, we will concentrate on radiation damage models able to reproduce the macroscopic effects of 3D and LGAD detectors.

3 TCAD radiation damage modeling schemes

Radiation damage significantly impacts the electrical performance of solid-state detectors regarding both static (I-V, C-V) and active (CCE) behaviors depending on the irradiation level. A thorough comprehension of the macroscopic effects related to damage is essential for formulating a physics-driven numerical modeling scheme with predictive capabilities for the electrical behavior of irradiated silicon sensors.

The development of a TCAD radiation damage model considers a series of defect states characterized by their type (i.e., donor or acceptor), concentration (related to the fluence by means of the introduction rate), energy level within the semiconductor bandgap, distribution (i.e., single level, uniform/gaussian band of defects), and capture cross-sections for electrons and holes.

The goal is to reproduce the effects of radiation damage rather than its causes. Therefore, the widely acknowledged approach within the scientific community is to select only a limited number of effective defect states. Recognizing the inherent complexity of defects in post-irradiated silicon, which would be computationally intractable for TCAD, the prevailing scientific method is to simplify reality through modeling. This strategy involves starting with simple models and progressively increasing their complexity to account for specific effects and behaviors. The literature presents many radiation damage modelling schemes, which differ in terms of defect description and are often tailored to specific datasets and devices. They can be divided into two categories: bulk models and combined bulk and surface models. The first category includes the EVL model (2 levels) [13, 14],

2025 JINST 20 C09006

KIT (Eber) (2 levels) [15], Folkestad (3 levels) [3] and the Hamburg Penta Trap Model (HPTM) (5 levels) [5]. The second category includes Delhi (2 levels+ 2 acceptor interface traps) [6] and the New University of Perugia model (3 bulk levels and 2 interface trap bands, one for donors and one for acceptors) [4, 16–19]. Delhi model has been developed in Silvaco TCAD, while all other models with Synopsys TCAD. These models have been validated up to fluences of $\sim 10^{16}\,n_{eq}/cm^2$. To extend the numerical models already developed to extreme fluences, it will be necessary to consider the modeling of impact ionization, dopant removal, carriers' mobility, and the accurate parameterization of carrier lifetime and trap dynamics. While described by SRH statistics, the specific defect parameters (e.g., introduction rates, capture cross-sections) exhibit complex, non-linear fluence dependencies at extreme irradiation levels, necessitating further investigation for predictive modeling. It is also important to emphasize that damage models can acquire predictive capabilities, but only if they are developed on physically meaningful foundations, and can reproduce experimental data across different devices and operating conditions. In this way, they can be used for detector design, development, and optimization before the actual manufacturing process, ultimately reducing time and costs. In the next section we will present the Folkestad model and its application to the simulation of 3D devices. Section 3.2 introduces the New University of Perugia Model and demonstrate its highly accurate simulation capabilities for LGAD devices.

3.1 3D detector simulations using the Folkestad model

Building upon the EVL existing model [13], an additional level was incorporated to enhance the reproduction of charge collection efficiency, and it is known as the Folkestad model [3]. The model is able to reproduce I-Vs, C-Vs and CCE up to fluences of the order of $8 \times 10^{15}\,n_{eq}/cm^2$. The model was validated for a temperature range from -38.1 to -31.1°C. It demonstrated good agreement with the I-Vs and CCE [20] of irradiated 3D detectors although it overestimates the breakdown voltage (V_{BD}) [21]. It had not yet been used to simulate C-V characteristics. New I-Vs up to 350 V were carried out to measure the breakdown along with C-V measurements at 500 Hz and 1 kHz, conducted on 3D devices using a computer-controlled parametric system. This is based on a semiautomatic probe station with a Keithley K707 switching matrix, Keithley SMU 236 and 237 for I-V measurements and an Agilent 4284A for high-frequency C-V measurements. To achieve better agreement in terms of I-Vs, C-Vs, and breakdown voltage, and to assess the sensitivity of measured macroscopic quantities to different model parameters, new simulations have been carried out. Small-pitch 3D pixel sensors, featuring pixel sizes of 50×50 and 25×100 μm^2 with one readout electrode (hereafter referred to as 50 × 50 - 1E and 25 ×100 - 1E), were measured and simulated.

The sensor layout is described in [21]. Vertical electrodes are etched by Deep Reactive Ion Etching (DRIE) from the front side. The p^+ electrodes penetrate into the handle wafer to allow for bias from the backside. The n^+ electrodes stop at a safety distance (gap = 30 µm) from the handle wafer to prevent early breakdown. A p-spray layer isolates the n^+ electrodes. The thickness of the active volume has been optimized in terms of signal amplitude and sensor capacitance, resulting in a value of 150 µm. The neutron irradiation was performed at the TRIGA Mark II reactor at the Jozef Stefan Institute (Ljubljana, Slovenia) with fluences of $1 \times 10^{16}\,n_{eq}/cm^2$ and $2.5 \times 10^{16}\,n_{eq}/cm^2$. The uncertainty in the neutron fluences is within 10%. Measurements have been carried out at -25°C. In figure 1a and 1b the I-V and C-V characteristics after a fluence of $1 \times 10^{16}\,n_{eq}/cm^2$ are shown, respectively. For the moment, we will concentrate on 50×50 device. The breakdown voltage is around 300–320 V and

2025 JINST 20 C09006

Table 1. Details of the Folkestad radiation damage modeling scheme.

	Acceptor	**Acceptor**	**Donor**
Energy [eV]	$E_V + 0.90$	$E_C - 0.525$	$E_V + 0.48$
η **[cm^{-1}]**	36	0.75	4
σ_e **[cm^2]**	1.0×10^{-16}	5.0×10^{-15}	2.0×10^{-14}
σ_h **[cm^2]**	1.0×10^{-16}	1.0×10^{-14}	1.0×10^{-14}

there is an increase of the current after the depletion near 170 V. The depletion voltage is in the range 85–90 V for the two measured diodes. Simulations have been carried out using the same simulation approach described in [21]. The simulations have been carried out at -38°C and then the current has been scaled using Chilingarov's formula [22]. Table 1 reports the original parameters' values of the Folkestad Model. The parameters of the Folkestad model have been analyzed and modified in order to obtain a better agreement in terms of I-Vs and C-Vs characteristics.

In particular, the introduction rate and the capture cross section of the donor $E_V + 0.48$ eV have been modified to obtain a better agreement in terms of I-V and depletion voltage. The depletion voltage was extracted from CV characteristics as the crossing of the extrapolated rising straight segment of the $1/C^2$ and the saturated value. Figure 2a shows the effect of the variation of the introduction rate (η) of the donor on the I-V after 1×10^{16} n_{eq}/cm^2. The increase of the η decreases the breakdown voltage, increasing the leakage current. Figure 2b shows that the effect of the increase of the capture cross section of the donor is similar. Figure 3a and figure 3b show the effect of the variation of these parameters on the C-V and the depletion voltage, respectively. Charge collection efficiency simulations will be carried out changing the different parameters to compare the simulated results with experimental ones obtained using a β source in collaboration with INFN of Torino. The analysis of the effect of the different parameters on I-V, breakdown voltage, C-Vs and CCE will help to modify the model in order to obtain a better agreement in terms of breakdown voltage, depletion voltage and CCE, without comprising the agreement in terms of I-V and C-V characteristics. The results of this analysis will be presented in a future work.

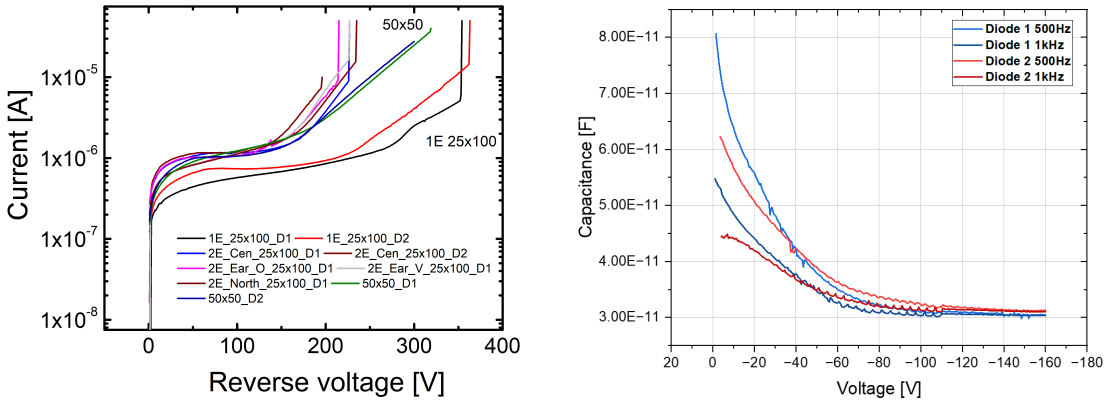

(a) (b)

Figure 1. (a) I-Vs measured at -25°C on different 3D layout irradiated at 1×10^{16} n_{eq}/cm^2. (b) C-V measured at 500 Hz and 1 kHz on 50×50 irradiated at 1×10^{16} n_{eq}/cm^2.

2025 JINST 20 C09006

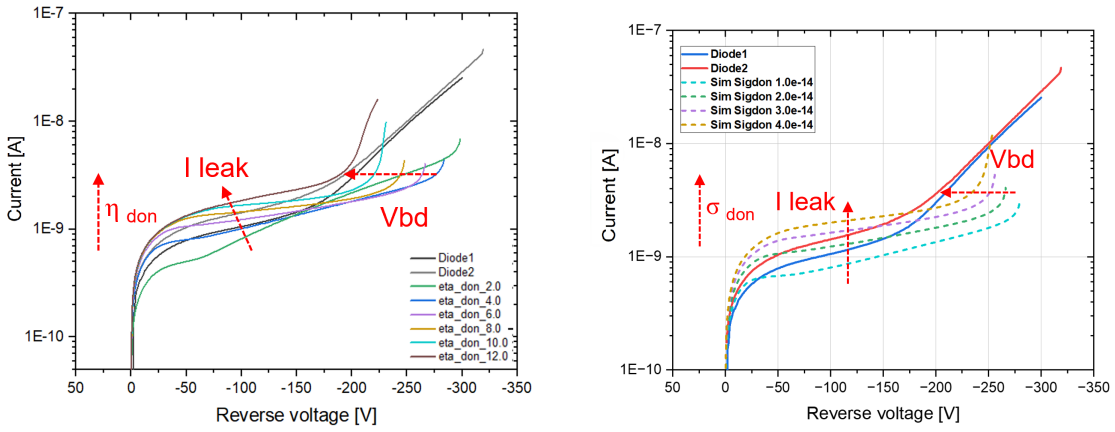

(a) (b)

Figure 2. Effect of the (a) introduction rate and (b) capture cross section of the donor trap state on I-Vs simulated at -25°C of 50×50 3D detectors irradiated at 1×10^{16} n_{eq}/cm^2.

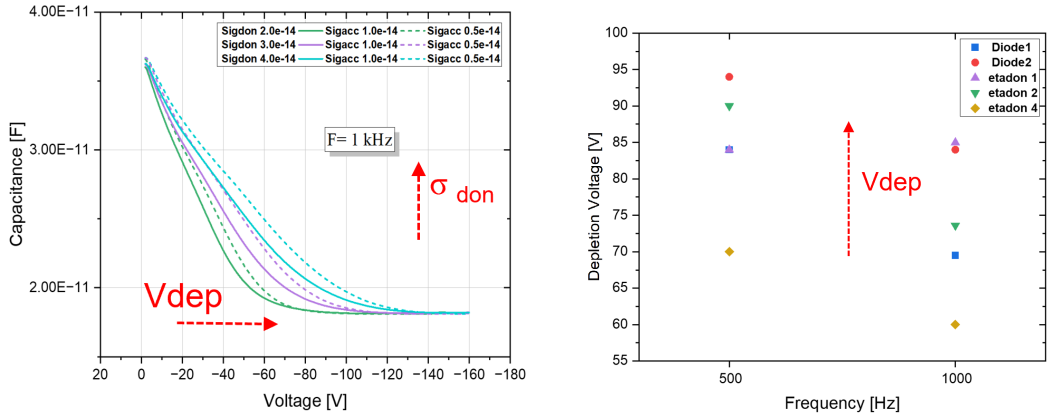

(a) (b)

Figure 3. (a) Effect of capture cross sections of donor and acceptor near midgap on C-V characteristics simulated at -25°C on 50×50 3D detectors irradiated at 1×10^{16} n_{eq}/cm^2. (b) Effect of η of donor on depletion voltage simulated at -25°C on 50×50 3D detectors irradiated at 1×10^{16} n_{eq}/cm^2.

3.2 LGAD device simulations using the New University of Perugia model

Recently, the *New University of Perugia* comprehensive numerical modeling scheme, that accounts for the combined effect of surface [18] and bulk radiation damage [23] on silicon detectors, has been updated. Indeed, the so called *Perugia Modified Doping* (PerugiaModDoping) TCAD radiation damage model [19, 24, 25] combines the traps parameterization of the *New University of Perugia* radiation damage model [4] with the fluence-dependent analytical parameterizations of the Gain Layer and bulk effective doping, called *Torino analytical parameterizations* [26]. As a consequence, both the acceptor-removal mechanism [27] and the saturation of the acceptor-creation mechanism [28] have been reliably considered, within the TCAD environment.

2025 JINST 20 C09006

This modelling scheme has been used to simulate the electrical behavior of Low Gain Avalanche Diodes. Figure 4a and 4b show the comparison between measurements and simulation results in terms of Current-Voltage (I-V) and Gain-Voltage (G-V) of non-irradiated and irradiated LGADs devices.

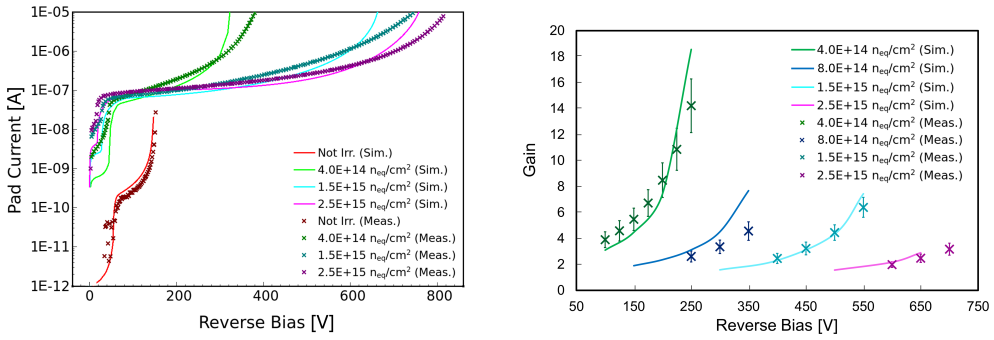

(a) (b)

Figure 4. (a) Simulated LGAD I-V compared to the measured one, before and after irradiation. "New University of Perugia" TCAD model. (b) Simulated LGAD gain compared to the measured one, before and after irradiation (fluence 1.5×10^{15} n_{eq}/cm^2). "New University of Perugia" TCAD model.

For the sake of robustness and to ensure the model's physical accuracy, we started from simulations of non-irradiated LGAD devices to meaningfully define the layout options, the manufacturing parameters and the non-ideal effects such as the oxide charges at Si/SiO_2 interfaces. The model validation relies on the comparison between measurements and simulations. Following successful validation of the model for non-irradiated devices, additional factors, such as the fluence-dependent parameterization of the radiation damage effects, can be considered. A measurement-driven approach guides the radiation damage modeling in this study, with the primary objective of creating models that accurately reproduce the macroscopic electrical characteristics observed experimentally. This involves using measurements to set the model's parameters, aiming for a physically sound representation. The model accurately reproduce the electrical characteristics of LGAD sensors in different operating conditions (i.e., temperature, frequency and irradiation level). The good agreement obtained between simulation results and experimental data allow us to apply the newly developed model for the optimization of compensated LGAD [29].

The gain layer in standard LGADs is made by a single acceptor dopant implant, which is almost completely deactivated at about 2.5×10^{15} n_{eq}/cm^2 due to the acceptor removal mechanism [26]. To maintain the multiplication layer up to higher fluences, a possible solution is to realize the gain layer as a superposition of two implants of opposite doping species (e.g. boron and phosphorus). The resulting effective doping is the net difference between boron and phosphorus densities, which, if properly engineered, is equal to the typically concentration found in standard LGADs. Both implants will undergo dopant removal due to irradiation; however, their difference will remain fairly constant (figure 5), thus guaranteeing full functionality of the compensated LGADs at the required fluences [29].

2025 JINST 20 C09006

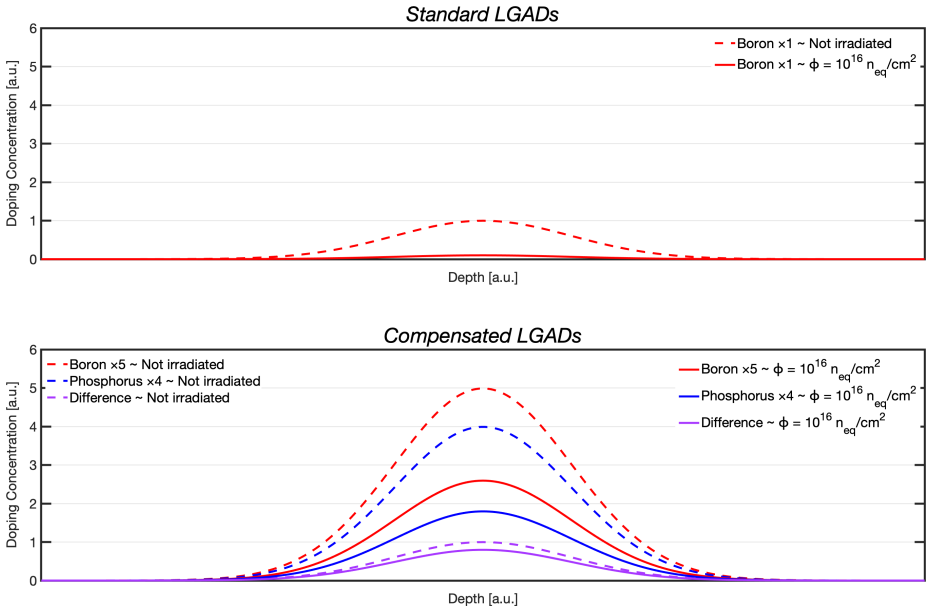

Figure 5. Evolution of the two gain layer designs (the standard one on the top row and the compensated one on the bottom row) with irradiation (unirradiated devices in dashed lines and irradiated ones in solid lines). The boron gain layer in standard LGADs becomes completely deactivated above around 2.5×10^{15} n_{eq}/cm^2 due to acceptor removal. Meanwhile, in compensated LGADs, the effective gain layer is almost unchanged by irradiation, although the individual implants experience acceptor and donor removal.

4 Extraction of doping removal coefficients by TCAD simulations

In order to realize compensated LGADs with gain layer still active at extreme fluences, it is necessary to investigate some still unresolved issues. First of all, it is necessary to know more about donor removal, since it has only been studied for low initial donor concentrations ($<10^{14}$ $1/cm^3$) and up to fluences of the order of 1×10^{14} n_{eq}/cm^2 [30]. Furthermore, it is necessary to understand if there is an interplay between donor and acceptor removals. Finally, it is crucial to understand if impurities such as oxygen and carbon continue to have beneficial effects in terms of dopant removal if both are present in the gain region. TCAD simulations can be helpful in understanding these phenomena, through the comparison between simulations results and measurements carried out on the first batch of compensated LGADs manufactured by FBK in 2022 [31]. Three different combinations of acceptor and donor doses were studied, 2−1, 3−2 and 5−4 where the first number is related to the number of standard doses of boron and the second to those of phosphorus, used by FBK for a standard implant. Finally, carbon was co-implanted in wafer 13, with a 3−2 combination to verify that it still reduces the acceptor removal coefficient even in the presence of a co-implantation of phosphorus.

To this end, the radiation damage has been taken into account by using the previously described Perugia radiation damage model [32]. This model parameterizes acceptor and donor removal as follows:

$$N_{A,D}(\phi) = N_{A,D}(0) \cdot e^{-c_{A,D} \cdot \phi}$$

where $c_{A,D}$ is the acceptor (donor) removal coefficient depending on the initial acceptor (donor) concentration $N_{A,D}(0)$, and ϕ is the irradiation fluence in n_{eq}/cm^2. The c_A values are known across a wide range of $N_A(0)$ based on studies of standard LGADs [26], while c_D values at high initial donor

2025 JINST 20 C09006

concentration (>10^{14} 1/cm^3) can be estimated by comparing C-V measurements and simulations. Specifically, it has started with the C-Vs of the wafer with 3 doses of boron and two of phosphorus (wafer 12), following the methodology reported in [33] and briefly summarised below:

1. Start with the simulation of non-irradiated device. The C-V measurements of p-i-n diodes can be used to calibrate the substrate thickness and doping concentration within the TCAD environment;

2. Gaussian fits derived from SIMS measurements of the compensated gain were incorporated into the TCAD environment. The agreement between C-V measurements and simulations before irradiation has been verified.

3. For a given initial acceptor concentration $N_{A_{\text{peak}}}(0)$ the acceptor removal parameter c_A is selected based on the established parametrization [26]. Subsequently, c_D is varied, guided by physical intuition regarding defect formation, until a satisfactory agreement is achieved between simulated and measured C-V characteristics after irradiation.

The removal coefficients that bring the simulations into agreement with the measurements are $c_A = 2.50 \times 10^{-16}$ cm^2 and $c_D = 6.50 \times 10^{-16}$ cm^2 [33]. We observed that $c_D \sim 2 \cdot c_A$ assuming both coefficients exhibiting the same dependence on the initial doping density ($N_{A,D}(0)$). This analysis considers the different initial concentrations of implanted boron and phosphorus.

The previously extracted value for c_D allows to achieve a good simulation-measurement agreement also for the wafer with co-implantated carbon. In this case, the c_A is 8.3×10^{-17} cm^2, which is one-third of the previous one, thus confirming the beneficial effect of carbon even when the phosphorus is co-implanted in the gain implant region.

A new method for investigating doping removal has been explored, specifically by observing changes in the sheet resistance through van der Pauw (vdP) structures [34], as a function of the irradiation. Van der Pauw test structures are four-terminal devices commonly used by foundries as standard tools for process quality control. By applying a current through two contacts and sensing the resulting voltage across the other two, it is possible to measure the sheet resistance. For the purpose at hand, measurements and simulations of vdP test structures have been compared. For the sake of completeness, a vdP test structure for each doping implant used in compensated LGADs was included in the batch, but we concentrate on the test structure to analyze the standard boron gain implant (figure 6).

Synopsys Sentaurus TCAD allows for the design of a vdP test structure within a 3D simulation domain, enabling the calculation of sheet resistance according to the measurement procedure. Thus, the doping variation with irradiation can be determined by tuning the doping profile in TCAD until it accurately reproduces the experimental change in sheet resistance with fluence. Moreover, for the p-type gain implant on a p-type substrate, the latter introduces a parasitic effect on the measured sheet resistance because the implanted layer and the substrate are not separated by a depletion region. However, TCAD simulation can accurately reproduce this parasitic contribution, allowing valuable information to be extracted by comparing measurements and simulations, particularly when considering the acceptor creation parametrization within the Perugia radiation damage model.

Figure 7a shows the simulated evolution of PGAIN profile with irradiation, which was used to reproduce the changes observed in the experimental sheet resistance (figure 7b). The black curve illustrates a process simulation calibrated considering SIMS profiles, while the post-irradiation curves

2025 JINST 20 C09006

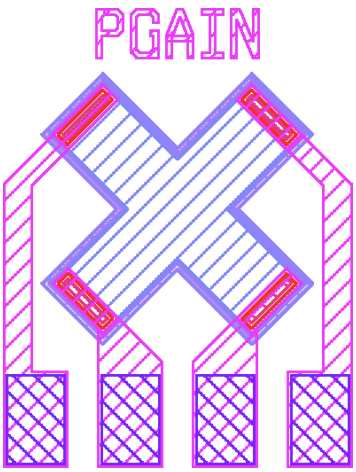

Figure 6. Layout of the van der Pauw test structure to study the implanted gain layer included in the first batch of Compensated LGADs released by FBK in late 2022.

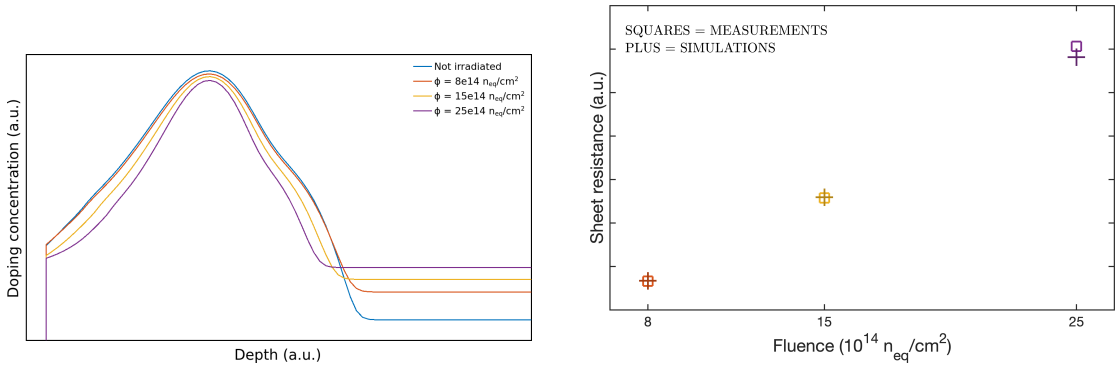

(a) (b)

Figure 7. (a) PGAIN doping profile evolution with irradiation. The substrate doping increases following the acceptor creation parametrisation, while the gain implant doping decreases accordingly to the acceptor removal parametrisation. (b) Pre- and post-irradiation sheet resistance measurements and simulations for the PGAIN implant.

have been derived by applying the acceptor removal (gain implant) and creation (substrate) models embedded in the Perugia radiation damage model. Figure 7b shows the very good agreement between simulations and measurements, showing the validity of the method for assessing doping removal. This approach can independently estimate the variation of each doping implant used in Compensated LGADs, utilising a dedicated van der Pauw test structure for each of them and therefore it will be applied to the new n-type LGAD batch currently in production at FBK.

5 Conclusions

Various TCAD models for describing radiation damage effects consider different numbers of defects with distinct parameters. This implies that there is no unique parameterization, and multiple models may be effective for different devices. In this contribution, two different available TCAD numerical models addressing bulk and surface radiation damage effects have been used for the optimization

2025 JINST 20 C09006

of devices, particularly 3D sensors and Low Gain Avalanche Diodes. A good agreement between measurements and simulations has been obtained in particular for LGAD devices, while for 3D detectors further analysis are in progress. The Perugia model parametrization has been used to optimize the design of LGAD devices and to extract doping removal coefficients. Precisely, the measurement-simulation comparison of C-V characteristics facilitated the study of donor removal in compensated gain layers, estimating a donor removal rate about twice that of acceptor removal, assuming the same dependence on the initial acceptor and donor concentration. Moreover, measurements and simulations of van der Pauw test structures before and after irradiation have been compared to validate the change in sheet resistance as a method for assessing doping removal. Presently, achieving a simulation modeling scheme capable of effectively describing the entire range of measurements for different devices remains a challenge. There is a pressing need to develop a versatile model applicable to various detectors and irradiation levels. This would facilitate a better understanding of the behavior of novel detectors and support design optimization efforts.

Acknowledgments

This project has received funding from the European Union's Horizon 2020 Research and Innovation Programme under GAs Nos 101004761 (AIDAinnova) and 101057511 (EURO-LABS), the European Union – Next Generation EU, Mission 4 Component 1 CUP D53D23002870001 (Comon-Sens), and the European Union (ERC, CompleX, 101124288). Views and opinions expressed are however those of the authors only and do not necessarily reflect those of the European Union or the European Research Council. Neither the European Union nor the granting authority can be held responsible for them.

References

[1] Sentaurus Device User Manual, https://www.synopsys.com/.

[2] Silvaco TCAD User Manual, https://silvaco.com/tcad/.

[3] Å. Folkestad et al., *Development of a silicon bulk radiation damage model for Sentaurus TCAD*, *Nucl. Instrum. Meth. A* **874** (2017) 94.

[4] D. Passeri and A. Morozzi, *TCAD radiation damage model*, AIDA-2020-D7.4 (2020).

[5] J. Schwandt et al., *A new model for the TCAD simulation of the silicon damage by high fluence proton irradiation*, in the proceedings of the *2018 IEEE Nuclear Science Symposium and Medical Imaging Conference*, Sydney, NSW, Australia (2018), p. 1–3 [DOI:10.1109/NSSMIC.2018.8824412] [arXiv:1904.10234].

[6] C. Jain et al., *Modeling of neutron radiation-induced defects in silicon particle detectors*, *Semicond. Sci. Technol.* **35** (2020) 045021.

[7] M. Moll, *Displacement damage in silicon detectors for high energy physics*, *IEEE Trans. Nucl. Sci.* **65** (2018) 1561.

[8] M. Moll, *Radiation damage in silicon particle detectors: Microscopic defects and macroscopic properties*, Ph.D. Thesis, Universität Hamburg (1999) [DESY-THESIS-1999-040].

[9] G. Kramberger, *Reasons for high charge collection efficiency of silicon detectors at HL-LHC fluences*, *Nucl. Instrum. Meth. A* **924** (2019) 192.

2025 JINST 20 C09006

[10] A. Morozzi et al., *Thin silicon sensors for extreme fluences: A doping compensation strategy*, *Nucl. Instrum. Meth. A* **1069** (2024) 169904.

[11] I. Pintiliie, G. Lindstroem, A. Junkes and E. Fretwurst, *Radiation Induced Point and Cluster-Related Defects with Strong Impact to Damage Properties of Silicon Detectors*, *Nucl. Instrum. Meth. A* **611** (2009) 52 [arXiv:0907.3050].

[12] C. Da Via, G.-F. Dalla Betta and S. Parker, *Radiation Sensors with Three-Dimensional Electrodes*, CRC Press, Boca Raton, U.S.A. (2019) [DOI:10.1201/9780429055324].

[13] V. Eremin et al., *Double peak electric field distortion in heavily irradiated silicon strip detectors*, *Nucl. Instrum. Meth. A* **535** (2004) 622.

[14] V. Eremin, E. Verbitskaya and Z. Li, *The origin of double peak electric field distribution in heavily irradiated silicon detectors*, *Nucl. Instrum. Meth. A* **476** (2002) 556.

[15] R. Eber, *Investigations of new Sensor Designs and Development of an effective Radiation Damage Model for the Simulation of highly irradiated Silicon Particle Detectors*, Ph.D. Thesis, Karlsruhe Institute of Technology (2013) [DOI:10.5445/IR/1000038403].

[16] F. Moscatelli et al., *Combined Bulk and Surface Radiation Damage Effects at Very High Fluences in Silicon Detectors: Measurements and TCAD Simulations*, *IEEE Trans. Nucl. Sci.* **63** (2016) 2716 [arXiv:1611.10138].

[17] D. Passeri, P. Ciampolini, G.M. Bilei and F. Moscatelli, *Comprehensive modeling of bulk-damage effects in silicon radiation detectors*, *IEEE Trans. Nucl. Sci.* **48** (2001) 1688.

[18] A. Morozzi, F. Moscatelli, T. Croci and D. Passeri, *TCAD Modeling of Surface Radiation Damage Effects: A State-Of-The-Art Review*, *Front. in Phys.* **9** (2021) 617322.

[19] P. Asenov et al., *TCAD modeling of bulk radiation damage effects in silicon devices with the Perugia radiation damage model*, *Nucl. Instrum. Meth. A* **1040** (2022) 167180.

[20] A. Boughedda et al., *Comparing different bulk radiation damage models in TCAD simulations of small-pitch 3D Si sensors*, 2021 *JINST* **16** C10006.

[21] J. Ye, A. Boughedda, D.M.S. Sultan and G.-F. Dalla Betta, *TCAD Analysis of Leakage Current and Breakdown Voltage in Small Pitch 3D Pixel Sensors*, *Sensors* **23** (2023) 4732.

[22] A. Chilingarov, *Temperature dependence of the current generated in Si bulk*, 2013 *JINST* **8** P10003.

[23] A. Morozzi, F. Moscatelli, D. Passeri and G.M. Bilei, *TCAD advanced radiation damage modeling in silicon detectors*, *PoS* **Vertex2019** (2020) 050.

[24] T. Croci et al., *TCAD optimization of LGAD sensors for extremely high fluence applications*, 2023 *JINST* **18** C01008.

[25] T. Croci et al., *TCAD simulations of non-irradiated and irradiated low-gain avalanche diodes and comparison with measurements*, 2022 *JINST* **17** C01022.

[26] M. Ferrero et al., *Radiation resistant LGAD design*, *Nucl. Instrum. Meth. A* **919** (2019) 16 [arXiv:1802.01745].

[27] M. Moll, *Acceptor removal — Displacement damage effects involving the shallow acceptor doping of p-type silicon devices*, *PoS* **Vertex2019** (2020) 027.

[28] V. Sola et al., *Next-generation tracking system for future hadron colliders*, *PoS* **Vertex2019** (2020) 034.

[29] V. Sola et al., *A compensated design of the LGAD gain layer*, *Nucl. Instrum. Meth. A* **1040** (2022) 167232 [arXiv:2209.00494].

2025 JINST 20 C09006

[30] R. Wunstorf et al., *Investigations of donor and acceptor removal and long term annealing in silicon with different boron/phosphorus ratios*, *Nucl. Instrum. Meth. A* **377** (1996) 228.

[31] V. Sola et al., *The first batch of compensated LGAD sensors*, *Nucl. Instrum. Meth. A* **1064** (2024) 169453.

[32] A. Morozzi et al., *TCAD simulations for radiation-tolerant silicon sensors*, *PoS* **VERTEX2023** (2024) 060.

[33] A. Fondacci et al., *TCAD investigation of Compensated LGAD Sensors for extreme fluence*, *Nucl. Instrum. Meth. A* **1068** (2024) 169811.

[34] L.J. van der Pauw, *A Method of Measuring Specific Resistivity and Hall Effect of Discs of Arbitrary Shape* in *Semiconductor Devices: Pioneering Papers*, World Scientific (1991), p. 174–182 [DOI:10.1142/9789814503464_0017].

2025 JINST 20 C09006